EUROPEAN ORGANIZATION FOR NUCLEAR RESEARCH

Letter of Intent to the ISOLDE and Neutron Time-of-Flight Committee

Measuring Interfacial Ionic Conductivity in All-Solid-State-Batteries with Li β-NMR Spectroscopy

26 September 2023

G. Rees[1,2], A. Sparks[3], N. Azaryan[3,4], M. Baranowski[4], M.L. Bissell[3], P. Bruce[1,2], M. Chojnacki[3,4], R. House[1,2], M. Jankowski[3,5], M. Kowalska[3,4], I. Michelon[3,4], N. Mitchell[1,2], M. Piersa-Silkowska[3], D. Paulitsch[3,6], B. Payne[1,2], Z. Salman[7], T. Treczoks[8], D. Zakoucky[9].

1 Department of Materials, University of Oxford, Oxford, UK.
2 The Faraday Institution, Didcot, UK.
3 Experimental Physics Department, CERN, Geneva, Switzerland
4 Department of Particle and Nuclear Physics, University of Geneva, Geneva, Switzerland
5 Institute for Nuclear Physics, Technical University Darmstadt, Darmstadt, Germany
6 University of Innsbruck, Innsbruck, Austria
7 University of Oldenburg, Oldenburg, Germany
8 Nuclear Physics Institute, Czech Academy of Sciences, Rez, Czechia
9 Nuclear Physics Institute, Czech Academy of Sciences, Rez, Czechia

Spokesperson: Gregory Rees (gregory.rees@materials.ox.ac.uk)
Co-spokesperson: Amy Sparks (amy.sparks@cern.ch)

Technical coordinator: Magdalena Kowalska (kowalska@cern.ch)

CERN-INTC-2023-078 / INTC-I-267
04/10/2023

Abstract

We request access to ^{8}Li beam for exploratory β-NMR experiments on solid-state battery (SSB) materials. SSBs are promising next-generation battery electrolyte, however, they currently suffer from low critical current densities (the amount of current that causes cell failure) and longer than expected charging times. Sluggish interfacial Li ion diffusion is expected be the cause of this poor performance, but it cannot be easily measured with sub-micron precision with the existing bulk experimental techniques. The aim of the present LOI is to investigate the performance and feasibility of the present β-NMR setup at the VITO beamline (high-vacuum, 4.7 T field, and room temperature studies with beams of 30-50 keV) in measuring Li ion diffusion inside representative SSB materials. Spin-lattice (T_1) relaxation time measurements, Larmor frequency, and resonance width will be used to determine the diffusion inside and across the different SSB layers. Based on the results, possible upgrades to the experimental setup will be envisaged and funding before these improvements will be applied for.

Requested shifts: [8] 8h shifts, split into 1-2 runs over 1 year
Experimental beamline: VITO

Introduction and motivation

Solid-state batteries (Li-SSBs) offer a potential route to address the poor range, slow charging, and safety issues associated with current Li-ion batteries in cars, by utilizing lithium metal anodes.[1] The use of a solid electrolyte instead of a volatile liquid one used in current lithium-ion batteries is also inherently safer. However, achieving commercial Li-SSBs is a multi-faceted problem with many limitations; one of which is the reduction in ionic conductivity as you go from liquid to solid electrolytes (~10^{-10} m^2s^{-1} to ~10^{-12} m^2s^{-1}).[2] This can limit the rate of charge and capacity of the electrochemical cell. As a result, materials, and methods for achieving high ionic conductivities in solid electrolytes are integral to commercialising Li-SSBs. Figure 1a shows a schematic typical configuration of an SSB with all the conductivity resistances present in these systems. The solid-state electrolyte is sandwiched between a lithium metal anode (which has the highest available energy density) and a single crystal lithium nickel manganese cobalt oxide (NMC) cathode (the most stable high-capacity cathode). When the electrodes are deposited onto the electrolyte they react and form interfaces with complicated chemical compositions.[3,4] On the anode side of the cell this interface is known as the solid-electrolyte interface (SEI) and on the cathode side, it is called the cathode-electrolyte interface (CEI), highlighted in Fig. 1a.

Our current understanding of ion transport mechanisms in solids is fractured due to the problems extrapolating ion migration processes on a local atomic length scale (nano-ionics) to those on a macroscopic length scale (macro-ionics). These problems are exacerbated by the lack of analytical techniques that can sample such large length and time scales. For example, one bond cation hops typically take place on Angstrom length scales and rapid timescales, whilst migration across grain boundaries and interfaces is typically over micrometre length scales and much longer timescales. To address this, we have developed a suite of magnetic resonance techniques, supported by impedance spectroscopy and quasi-elastic neutron scattering (QENS), that can quantify ionic diffusion over varying length and time scales. This methodology is illustrated in Fig. 1b with example data given for Li_6PS_5Cl given in Fig. 1c. From this, we can determine which length scale and feature have the greatest diffusion resistance. This allows us to create new synthetic or processing steps to improve the overall conductivity of the materials. For example, if the macroscopic length scales are found to have large diffusion resistances then methods to improve particle-particle interactions or increase the distance between grain boundaries are targetted (such as sintering). One limitation of this methodology is that the techniques used in Fig. 1b are all bulk-sensitive and do not give any information about the interfaces.

One of the most promising solid electrolytes is the argyrodite Li_6PS_5Cl (LPSCl). It can be synthesized through solution-based methods, ideal for scale-up production, and forms a stable interface with Li metal anodes. On top of this, it has shown promising ionic conductivities of 3-4 mS/cm (1-3 x 10^{-12} m^2s^{-1}).[5] Currently, there are no methods to measure diffusion at the SEI and CEI interfaces in these argyrodite solid-state batteries. This is critical as it is where the electrolyte and anode will react to form undesirable side products, that are predicted to have lower diffusion coefficients.[6] From previous work, using *in-situ* XPS and time-resolved impedance spectroscopy, the stability and interphase growth of the argyrodite-type compounds Li_6PS_5Cl in contact with Li metal was investigated.[7] The XPS results show that Li_2S and Li_3P form together with LiCl and electrolytes that do not contain Cl have a lower resistivity at the interface. Conversely, using time-of-flight secondary ion mass spectrometry (ToF-SIMS), Otto has suggested that a Li_2S-rich interface forms between the metal anode and the sulphide argyrodite with a thickness of ~250 nm.[8] As Li_2S has a conductivity that is ten orders of magnitude lower than Li_6PS_5Cl[9], this interface is expected to be the bottleneck for effective lithium-ion transfer through the cell. One route to reduce this sulphide-rich interface is to use a more chlorine-rich analogue of the argyrodite, $Li_{5.5}PS_{4.5}Cl_{1.5}$. This Cl-rich analogue also has a

superior bulk ionic conductivity (3 Vs 8 mS/cm as shown in Fig. 2a with ionic conductivities of 3 Vs 8 x10^{-12} m^2s^{-1}).[2] However, as shown in Fig. 2b, this x2.5 increase in conductivity gives no appreciable increase in full-cell performance. Both the Li_6PS_5Cl and $Li_{5.5}PS_{4.5}Cl_{1.5}$ have very similar critical current densities (the maximum current that can pass through the cell before short circuits take place) of ~0.8 and ~1 mA cm^{-2}, respectively. This confusion about whether a sulphur-rich or chlorine-rich interface is desirable, highlights our need to have a probe to measure the diffusion of the interface. This will allow us to tailor the chemistry of the anode/cathode interface and maximise Li-ion diffusion giving greater critical current densities leading to faster charging batteries.

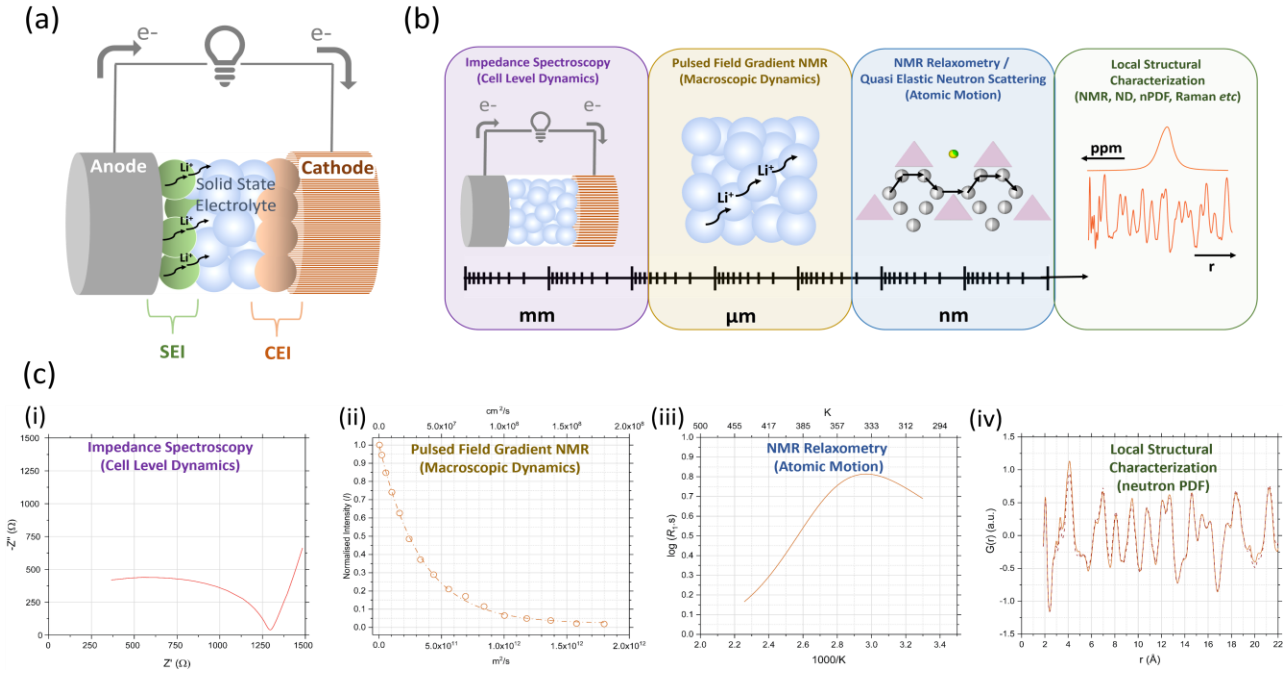

Figure 1: (a) A schematic of an all-solid-state battery, that consists of a metallic lithium anode, single crystal lithium nickel manganese cobalt oxide (NMC) cathode sandwiching an argyrodite Li_6PS_5Cl electrolyte. As these electrochemical cells are pressed together the cathode and anode react with the solid-state electrolyte forming interfaces known as the cathode-electrolyte interface (CEI, orange) and a solid anode-electrolyte interface (SEI, green), respectively. (b) A typical workflow for measuring lithium ion dynamics in battery materials over different length scales. These methods are all bulk and are therefore biased by the main conductive process. This means that the conductivity of the interfaces is not measured in these experiments. (c) The (i) impedance spectroscopy, (ii) pulsed field gradient (PFG) nuclear magnetic resonance (NMR), (iii) temperature-dependant spin-lattice relaxation, and (iv) local structural neutron pair distribution function (nPDF) characterisation of a Li_6PS_5Cl solid-state electrolyte. This bulk-sensitive workflow allows us to determine that changes to the local structure will have the greatest effect on Li-ion diffusion.

β-NMR technique and experimental setup

The VITO beamline as it will be used for this LOI is shown in Fig 2. It features a 4.7 T magnet, 1e-6 mbar vacuum and room temperature β-NMR chamber. It has been already used for liquid and solid β-NMR studies on several Na and K isotopes.

In this project, we will use laser polarised ^{8}Li (t1/2 = 840 ms), which has been polarised and used extensively by some of us in solid hosts at the ISOLDE COLLAPS.[10,11] Lithium-8 is easily polarised, exhibits a relatively high beta-decay asymmetry (in the range of 5-10%), and exhibits relatively long relaxation times in many solid hosts (comparable to its half-life). As in the COLLAPS experiments, at VITO the beam will be polarised in the atomic D1 or D2 line at 671 nm, which will be provided by a Ti:Sa laser hosted in a laser lab in bldg. 508. The light will be guided to the beamline via an optical fibre.

Since the magnetic moment of ^{8}Li is very well known, we will set up the NMR rf circuit into resonance with the expected Larmor frequency at 4.7 T. The new VITO time resolved DAQ system will be used to record data and for offline analysis.

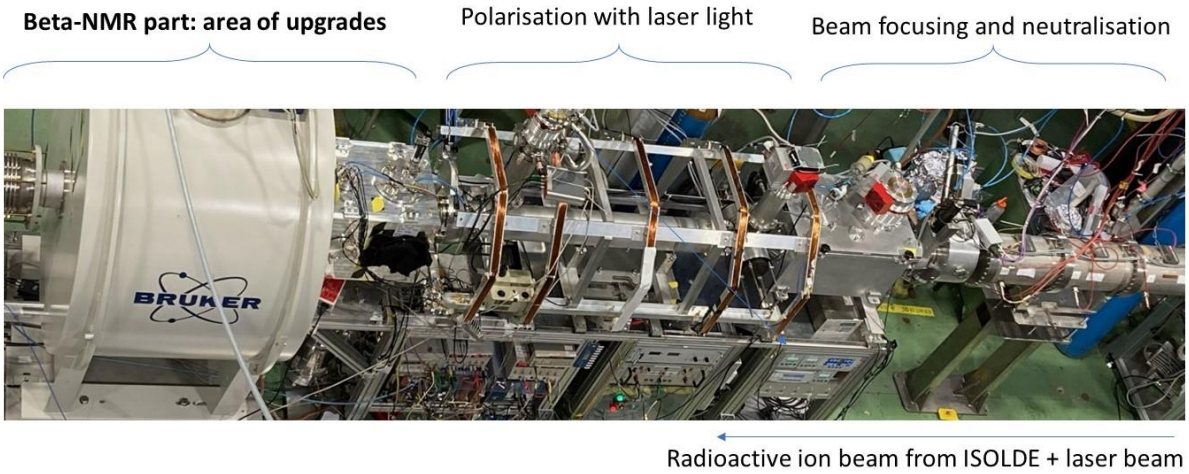

Fig. 2 VITO setup at ISOLDE. The exploratory measurements will take place using laser polarised 8Li beam inside a 4.7 T magnet at 1e-6 mbar pressure and at room temperature.

Envisaged exploratory β-NMR Dynamics Studies

For the first time, utilizing β-NMR, we aim to measure the diffusion coefficient and the microscopic activation energies of ^{8}Li ions in the CEI and SEI. We plan to use commercially relevant electrochemical cells with varying nickel-content NMC cathodes and lithium metal anodes. These electrodes will be separated by three electrolytes with changeable chlorine/sulphur content; $Li_7P_3S_{11}$ (LPS), Li_6PS_5Cl (LPSCl) and $Li_{5.5}PS_{4.5}Cl_{1.5}$ (Cl-rich).

We aim to use spin-lattice (T_1) relaxation to determine the dynamics and corresponding activation energy for microscopic ion migration in solid-state electrolytes.[12–14] R_1 ($1/T_1$) is sensitive to Li-ion jump rates that are proportional to the Larmor frequency (MHz, 10^9 s^{-1}). Therefore, relaxation rates are sensitive to fluctuations in the local nuclear environments occurring on timescales that are the inverse of the NMR Larmor frequency. The resultant data can be fitted to the Bloembergen, Purcell, and Pound (BPP) model ($J(\omega_0\tau) \propto C\frac{2\tau}{1+(\omega_0\tau)^2}$). The temperature-dependent values for relaxation rate (R_1) pass through a maximum when the time scales for fluctuations in local interactions are on the order of the Larmor frequency ($\omega_L\tau_c \approx 0.62$). The resultant Lorentzian peak is typically asymmetrical due to correlation effects such as Coulombic interactions and disorder affecting the low-temperature flank. In the high-temperature regime, in a three-dimensional isotropic ion conductor where $\omega_0\tau \ll 1$, such as Li_6PS_5Cl, the activation energy ($E_{a(HT)}$) for long-range ion motion is observed. An example of this using bulk-sensitive ^{7}Li NMR is given in Fig. 1c (iii).[15] Moreover, hyperpolarised ^{8}Li β-NMR is a surface-sensitive technique allowing us to specifically probe the dynamics near the electrode-electrolyte interfaces.

Anode SEI Formation

Through physical vapour deposition (PVD), a set of commercially relevant electrolytes will have three different thicknesses of lithium metal added to their surface (9 samples with SEIs and 3 standard electrolytes, giving 12 samples in total, outlined in Table 1 and schematic Fig. 2c). The metallic anode thicknesses will be 25 nm, 150 nm, and 200nm. Figure 2d shows an atomic force microscopy (AFM) line scan of an LPSCl electrolyte with 150 nm of lithium metal deposited on its surface. The rationale for using variable thicknesses of the anode is that this ensures that the insertion of ^{8}Li is

surface-specific and varied. ^{8}Li is expected to be inserted into the material at a maximum depth of ~ 250 nm. The ^{8}Li will exchange with both the metallic anode and the electrolyte, the metal has a Knight shift of 260 ppm whilst the electrolyte appears at 3 ppm, meaning they can be readily distinguished with a modest magnetic field homogeneity (10s ppm). As β-NMR is a depth-specific technique, varying the anode thickness will allow us to probe different depths of the electrolyte. The electrolyte with no anode can be compared to the bulk-specific probes outlined in Fig. 1, whilst the 200 nm anode will mean the ^{8}Li only exchanges with ~50 nm of the electrolyte making it electrode-SEI specific. As noted previously, the expected thickness of the SEI is 250 nm.[8] Using conventional NMR methods it is not possible to achieve a signal from a 250 nm SEI in a 1 mm thick battery, as the SEI represents ~0.025 % of the NMR signal. However, the depth selectivity combined with hyperpolarisation of β-NMR means the experiments outlined above are SEI-specific.

Table 1: The electrolyte compositions, anode thicknesses and expected SEI depth probe using ^{8}Li β-NMR.

Electrolyte	Li metal Anode Thickness (nm)	Expected SEI depth probed (nm)
$Li_7P_3S_{11}$ (LPS)	No anode	250
	25	225
	150	100
	200	50
Li_6PS_5Cl (LPSCl)	No anode	250
	25	225
	150	100
	200	50
$Li_{5.5}PS_{4.5}Cl_{1.5}$ (Cl-rich)	No anode	250
	25	225
	150	100
	200	50

Complementary, X-ray photoelectron spectroscopy (XPS, Diamond Light Source) and neutron reflectometry (ISIS) are currently underway to determine the exact composition of the SEI. This will allow us to compare the achieved diffusion coefficients and activation energies with the chemical composition and degradation products.

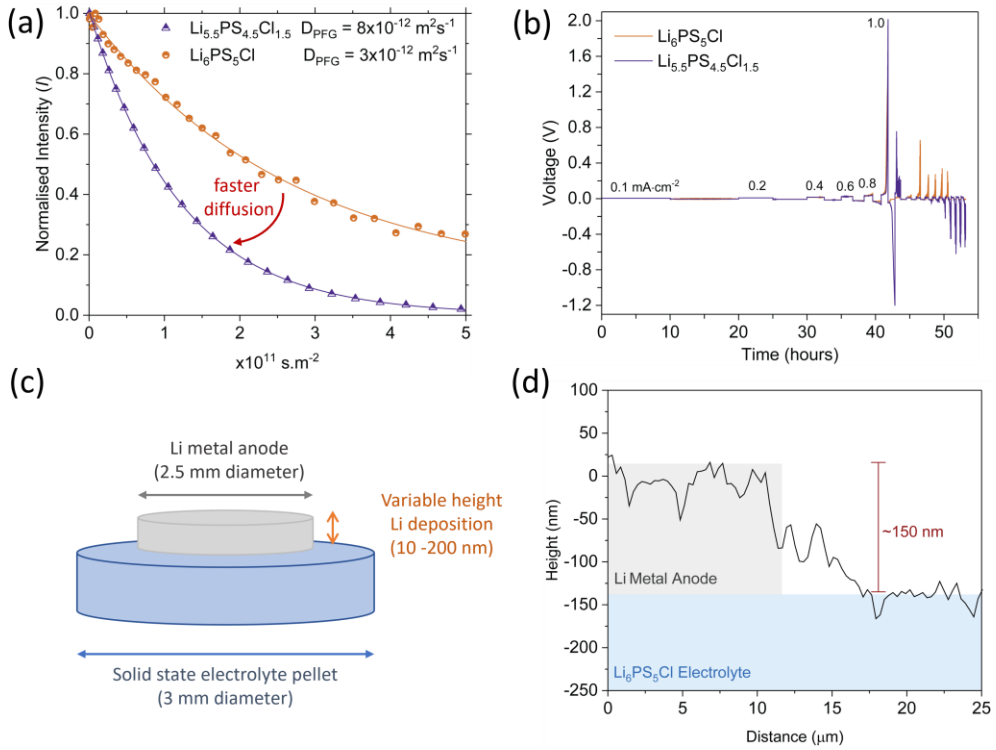

Figure 2: (a) The ^{7}Li pulsed field gradient (PFG) stimulated echo NMR determined macroscopic diffusion coefficients of Li_6PS_5Cl and $Li_{5.5}PS_{4.5}Cl_{1.5}$. The ^{7}Li diffusion coefficient for the Cl-rich analogue of the argyrodite is 2.5x greater than that of the stoichiometric material. (b) Despite this significant improvement in macroscopic diffusion the critical current density, the current at which the electrochemical cell fails is similar for both materials (~1 mA cm^{-2} using an NMC cathode and Li metal anode). This suggests that the bulk conductivity of the electrolyte has very little effect on the cell performance. (c) A schematic showing the electrolytes and variable anode thicknesses for the proposed β-NMR experiments. (d) Atomic force microscopy line scan of a Li_6PS_5Cl electrolyte with 150 nm of Li metal anode physically vapour deposited on the surface.

Beamtime request

We request an ^{8}Li beam from a Ta target and surface ioniser. We expect min 1e8 ions/s. We would like to make use of continuous and bunched ejection from the ISCOOL; thus we require to use the HRS target.

We estimate the following time needed for the measurements:

Establishing and optimising ^{8}Li polarisation and β-decay asymmetry at VITO = 1 shift

Establishing ^{8}Li NMR signal = 1 shift

Sample change (breaking vacuum, sample change, pumping) = 0.5 – 1 shift

Measuring T_1 in 1 sample = 1 hour

Measuring NMR resonances in 1 sample = 3 hours

To investigate 3 different reference samples (see Table 1) with 4 different thicknesses of the front layer (Table 2), resulting in 6 shifts required for measurements alone.

Because we expect to complete multiple sample changes (every few hours) and it takes time to reach the required 1e-6 mbar pressure in the experimental chamber, we request that the 2+6 shifts are split in 1-2 runs, each over the period of 4-5 days, and we possibly share the beam or the protons with other users.

References:

(1) Janek, J.; Zeier, W. G. A Solid Future for Battery Development. *Nat. Energy* **2016**, *1* (9), 1–4. https://doi.org/10.1038/nenergy.2016.141.

(2) Adeli, P.; Bazak, J. D.; Park, K. H.; Kochetkov, I.; Huq, A.; Goward, G. R.; Nazar, L. F. Boosting Solid-State Diffusivity and Conductivity in Lithium Superionic Argyrodites by Halide Substitution. *Angew. Chem.* **2019**, *131* (26), 8773–8778. https://doi.org/10.1002/ange.201814222.

(3) Peled, E.; Menkin, S. Review—SEI: Past, Present and Future. *J. Electrochem. Soc.* **2017**, *164* (7), A1703. https://doi.org/10.1149/2.1441707jes.

(4) Shan, X.; Zhong, Y.; Zhang, L.; Zhang, Y.; Xia, X.; Wang, X.; Tu, J. A Brief Review on Solid Electrolyte Interphase Composition Characterization Technology for Lithium Metal Batteries: Challenges and Perspectives. *J. Phys. Chem. C* **2021**, *125* (35), 19060–19080. https://doi.org/10.1021/acs.jpcc.1c06277.

(5) Zhang, Z.; Zhang, L.; Liu, Y.; Yan, X.; Xu, B.; Wang, L. One-Step Solution Process toward Formation of Li6PS5Cl Argyrodite Solid Electrolyte for All-Solid-State Lithium-Ion Batteries. *J. Alloys Compd.* **2020**, *812*, 152103. https://doi.org/10.1016/j.jallcom.2019.152103.

(6) Guan, P.; Liu, L.; Lin, X. Simulation and Experiment on Solid Electrolyte Interphase (SEI) Morphology Evolution and Lithium-Ion Diffusion. *J. Electrochem. Soc.* **2015**, *162* (9), A1798. https://doi.org/10.1149/2.0521509jes.

(7) Wenzel, S.; Sedlmaier, S. J.; Dietrich, C.; Zeier, W. G.; Janek, J. Interfacial Reactivity and Interphase Growth of Argyrodite Solid Electrolytes at Lithium Metal Electrodes. *Solid State Ion.* **2018**, *318*, 102–112. https://doi.org/10.1016/j.ssi.2017.07.005.

(8) Otto, S.-K.; Riegger, L. M.; Fuchs, T.; Kayser, S.; Schweitzer, P.; Burkhardt, S.; Henss, A.; Janek, J. In Situ Investigation of Lithium Metal–Solid Electrolyte Anode Interfaces with ToF-SIMS. *Adv. Mater. Interfaces* **2022**, *9* (13), 2102387. https://doi.org/10.1002/admi.202102387.

(9) Lin, Z.; Liu, Z.; Dudney, N. J.; Liang, C. Lithium Superionic Sulfide Cathode for All-Solid Lithium–Sulfur Batteries. *ACS Nano* **2013**, *7* (3), 2829–2833. https://doi.org/10.1021/nn400391h.

(10) Borremans, D.; Balabanski, D. L.; Blaum, K.; Geithner, W.; Gheysen, S.; Himpe, P.; Kowalska, M.; Lassen, J.; Lievens, P.; Mallion, S.; Neugart, R.; Neyens, G.; Vermeulen, N.; Yordanov, D. New Measurement and Reevaluation of the Nuclear Magnetic Andquadrupole Moments of $^{8}\mathrm{Li}$ and $^{9}\mathrm{Li}$. *Phys. Rev. C* **2005**, *72* (4), 044309. https://doi.org/10.1103/PhysRevC.72.044309.

(11) Neugart, R.; Balabanski, D. L.; Blaum, K.; Borremans, D.; Himpe, P.; Kowalska, M.; Lievens, P.; Mallion, S.; Neyens, G.; Vermeulen, N.; Yordanov, D. T. Precision Measurement of $^{11}\mathrm{Li}$ Moments: Influence of Halo Neutrons on the $^{9}\mathrm{Li}$ Core. *Phys. Rev. Lett.* **2008**, *101* (13), 132502. https://doi.org/10.1103/PhysRevLett.101.132502.

(12) Wilkening, M.; Heitjans, P. From Micro to Macro: Access to Long-Range Li+ Diffusion Parameters in Solids via Microscopic 6, 7Li Spin-Alignment Echo NMR Spectroscopy. *ChemPhysChem* **2012**, *13* (1), 53–65. https://doi.org/10.1002/cphc.201100580.

(13) Kuhn, A.; Kunze, M.; Sreeraj, P.; Wiemhöfer, H.-D.; Thangadurai, V.; Wilkening, M.; Heitjans, P. NMR Relaxometry as a Versatile Tool to Study Li Ion Dynamics in Potential Battery Materials. *Solid State Nucl. Magn. Reson.* **2012**, *42*, 2–8. https://doi.org/10.1016/j.ssnmr.2012.02.001.

(14) Hanghofer, I.; Gadermaier, B.; Wilkening, H. M. R. Fast Rotational Dynamics in Argyrodite-Type Li6PS5X (X: Cl, Br, I) as Seen by 31P Nuclear Magnetic Relaxation—On Cation–Anion Coupled Transport in Thiophosphates. *Chem. Mater.* **2019**, *31* (12), 4591–4597. https://doi.org/10.1021/acs.chemmater.9b01435.

(15) Heitjans, P.; Schirmer, A.; Indris, S. NMR and β-NMR Studies of Diffusion in Interface-Dominated and Disordered Solids. In *Diffusion in Condensed Matter: Methods, Materials, Models*; Heitjans, P., Kärger, J., Eds.; Springer: Berlin, Heidelberg, 2005; pp 367–415. https://doi.org/10.1007/3-540-30970-5_9.

(16) Lv, Y.; Huang, S.; Zhao, Y.; Roy, S.; Lu, X.; Hou, Y.; Zhang, J. A Review of Nickel-Rich Layered Oxide Cathodes: Synthetic Strategies, Structural Characteristics, Failure Mechanism, Improvement Approaches and Prospects. *Appl. Energy* **2022**, *305*, 117849. https://doi.org/10.1016/j.apenergy.2021.117849.

(17) Walther, F.; Koerver, R.; Fuchs, T.; Ohno, S.; Sann, J.; Rohnke, M.; Zeier, W. G.; Janek, J. Visualization of the Interfacial Decomposition of Composite Cathodes in Argyrodite-Based All-Solid-State Batteries Using Time-of-Flight Secondary-Ion Mass Spectrometry. *Chem. Mater.* **2019**, *31* (10), 3745–3755. https://doi.org/10.1021/acs.chemmater.9b00770.

(18) Zuo, T.-T.; Walther, F.; Teo, J. H.; Rueß, R.; Wang, Y.; Rohnke, M.; Schröder, D.; Nazar, L. F.; Janek, J. Impact of the Chlorination of Lithium Argyrodites on the Electrolyte/Cathode Interface in Solid-State Batteries. *Angew. Chem. Int. Ed.* **2023**, *62* (7), e202213228. https://doi.org/10.1002/anie.202213228.

(19) Koerver, R.; Walther, F.; Aygün, I.; Sann, J.; Dietrich, C.; Zeier, W. G.; Janek, J. Redox-Active Cathode Interphases in Solid-State Batteries. *J. Mater. Chem. A* **2017**, *5* (43), 22750–22760. https://doi.org/10.1039/C7TA07641J.

(20) Nakamura, K.; Ohno, H.; Okamura, K.; Michihiro, Y.; Nakabayashi, I.; Kanashiro, T. On the Diffusion of Li+ Defects in LiCoO2 and LiNiO2. *Solid State Ion.* **2000**, *135* (1), 143–147. https://doi.org/10.1016/S0167-2738(00)00293-9.

Appendix

DESCRIPTION OF THE PROPOSED EXPERIMENT

Please describe here below the main parts of your experimental set-up:

Part of the experiment	Design and manufacturing
VITO	☒ To be used without any modification ☐ To be modified
If relevant, describe here the name of the flexible/transported equipment you will bring to CERN from your Institute [Part 1 of experiment/ equipment]	☐ Standard equipment supplied by a manufacturer ☐ CERN/collaboration responsible for the design and/or manufacturing
[Part 2 experiment/ equipment]	☐ Standard equipment supplied by a manufacturer ☐ CERN/collaboration responsible for the design and/or manufacturing
[insert lines if needed]	

HAZARDS GENERATED BY THE EXPERIMENT

Additional hazard from flexible or transported equipment to the CERN site:

Domain	Hazards/Hazardous Activities		Description
Mechanical Safety	Pressure	☐	[pressure] [bar], [volume][l]
	Vacuum	☐	
	Machine tools	☐	
	Mechanical energy (moving parts)	☐	
	Hot/Cold surfaces	☐	
Cryogenic Safety	Cryogenic fluid	☐	[fluid] [m^3]
Electrical Safety	Electrical equipment and installations	☐	[voltage] [V], [current] [A]
	High Voltage equipment	☐	[voltage] [V]
Chemical Safety	CMR (carcinogens, mutagens and toxic to reproduction)	☐	[fluid], [quantity]
	Toxic/Irritant	☐	[fluid], [quantity]

	Corrosive	☐	[fluid], [quantity]
	Oxidizing	☐	[fluid], [quantity]
	Flammable/Potentially explosive atmospheres	☐	[fluid], [quantity]
	Dangerous for the environment	☐	[fluid], [quantity]
Non-ionizing radiation Safety	Laser	☐	[laser], [class]
	UV light	☐	
	Magnetic field	☐	[magnetic field] [T]
Workplace	Excessive noise	☐	
	Working outside normal working hours	☐	
	Working at height (climbing platforms, etc.)	☐	
	Outdoor activities	☐	
Fire Safety	Ignition sources	☐	
	Combustible Materials	☐	
	Hot Work (e.g. welding, grinding)	☐	
Other hazards			